

${}^2E(X) = {}^2E(Y) = {}^2E(2) = 4B - C$. With this assumption,

$$\eta_4 = \eta_5 = \frac{\zeta}{3\sqrt{2}} \left\{ \frac{1}{E({}^4E)} - \frac{1}{E({}^2E(2))} \right\}$$

From the above expressions for the Kramer's doublet, the equations for g_{\parallel} , g_{\perp} , A_{\parallel} , and A_{\perp} , correct to first order, are found to be:

$$g_{\parallel} = 2 \quad (1)$$

$$g_{\perp} = 2 - \frac{6\zeta}{E({}^2E(1))} \quad (2)$$

$$A_{\parallel} = -K + \frac{P}{7} \left\{ 4 + \frac{6\zeta}{E({}^2E(1))} + 4\zeta \left[\frac{1}{E({}^4E)} - \frac{1}{E({}^2E(2))} \right] \right\} \quad (3)$$

$$A_{\perp} = -K - \frac{P}{7} \left[2 + \frac{45\zeta}{E({}^2E(1))} \right] \quad (4)$$

where $K = P\kappa$.

The second-order equation for g_{\parallel} calculated from the formula, $2(+|Lz + 2Sz|+)$, turned out to be independent of the energies of 4A_2 and 2A_2 although the first-order expression for the Kramer's doublet contains them. Additional second-order contribution to g_{\parallel} comes from second-order state functions. The complete second-order equation for g_{\parallel} turns out to be dependent on the energy of ${}^2A_2(V)$. Thus,

$$g_{\parallel} = 2 - \frac{3\zeta^2}{\{E({}^2E(1))\}^2} + 2\zeta^2 \left[\frac{1}{\{E({}^4E)\}^2} - \frac{1}{\{E({}^2E(2))\}^2} \right] + \frac{8\zeta^2}{3E({}^2A_2(V))} \left[\frac{1}{E({}^4E)} - \frac{1}{E({}^2E(2))} \right] \quad (5)$$

The zeroth-order energies in these equations are functions of the Racah parameters, B and C , and the ligand field parameters, V_1 , V_2 , and V_3 . Besides these, K and P , corresponding to the isotropic and the anisotropic nuclear hyperfine interactions, are also unknown. When the covalency effect is not large we may use the free ion values for B , C , P , and ζ , and calculate K , V_1 , V_2 , and V_3 . Although admittedly the orbital energies thus calculated are only approximate, it is nevertheless well known that for porphyrin complexes, where d-d transitions are masked by strong π - π^* transitions, such information could not be obtained through other means, such as optical studies.

References and Notes

- (1) J. M. Assour, *J. Am. Chem. Soc.*, **87**, 4701 (1965).
- (2) F. A. Walker, *J. Am. Chem. Soc.*, **92**, 4235 (1970).
- (3) F. R. Longo, M. G. Finarelli, and J. B. Kim, *J. Heterocycl. Chem.*, **6**, 927 (1969).
- (4) A. D. Adler, F. R. Longo, F. Kamps, and J. B. Kim, *J. Inorg. Nucl. Chem.*, **32**, 2443 (1970).
- (5) J. S. Griffith, *Discuss. Faraday Soc.*, **26**, 81 (1958).
- (6) A. J. Freeman and R. E. Watson, "Magnetism II", G. T. Rado and H. Suhl, Ed., Academic Press, New York, N.Y., 1965, p 167.
- (7) H. A. Skinner and F. H. Sumner, *J. Inorg. Nucl. Chem.*, **4**, 245 (1957); J. S. Griffith, "The Theory of Transition-Metal Ions", Cambridge University Press, London, 1961, p 437.
- (8) T. M. Dunn, *Trans. Faraday Soc.*, **57**, 1441 (1961).
- (9) P. W. Lau and W. C. Lin, *J. Inorg. Nucl. Chem.*, **37**, 2389 (1975).
- (10) M. C. R. Symons and J. G. Wilkinson, *J. Chem. Soc.*, 2069 (1971).
- (11) J. Otsuka, *J. Phys. Soc. Jpn.*, **21**, 596 (1966).

Intramolecular Ligand Exchange in Phosphoranes. A Comparison of Berry Pseudorotation and Turnstile Rotation

Julianna A. Altmann, Keith Yates,* and I. G. Csizmadia

Contribution from the Department of Chemistry, University of Toronto, Toronto, Ontario, Canada M5S 1A1. Received April 22, 1975

Abstract: Ab initio calculations employing a large basis set have been carried out for a model molecule (PH_5) to investigate the reaction profiles corresponding to the Berry pseudorotation (BPR) and the turnstile rotation (TR), these being the mechanistic possibilities proposed for the intramolecular ligand exchange in phosphoranes. Results suggest that the BPR should be a concerted process involving a very low (1.95 kcal/mol) energy of activation. In contrast, the TR process, which could be the active reaction coordinate for structurally restricted systems, may be better described as a sequential type process with a considerably larger (10.05 kcal/mol) overall activation energy. Examination of the reaction hypersurface in the vicinity of the C_2 and C_{4v} points revealed that only the C_{4v} geometry represents a genuine saddle point. This implies that, at least in the case of structurally flexible phosphoranes as modeled by PH_5 , the TR should be regarded as a vibrationally excited mode of the BPR.

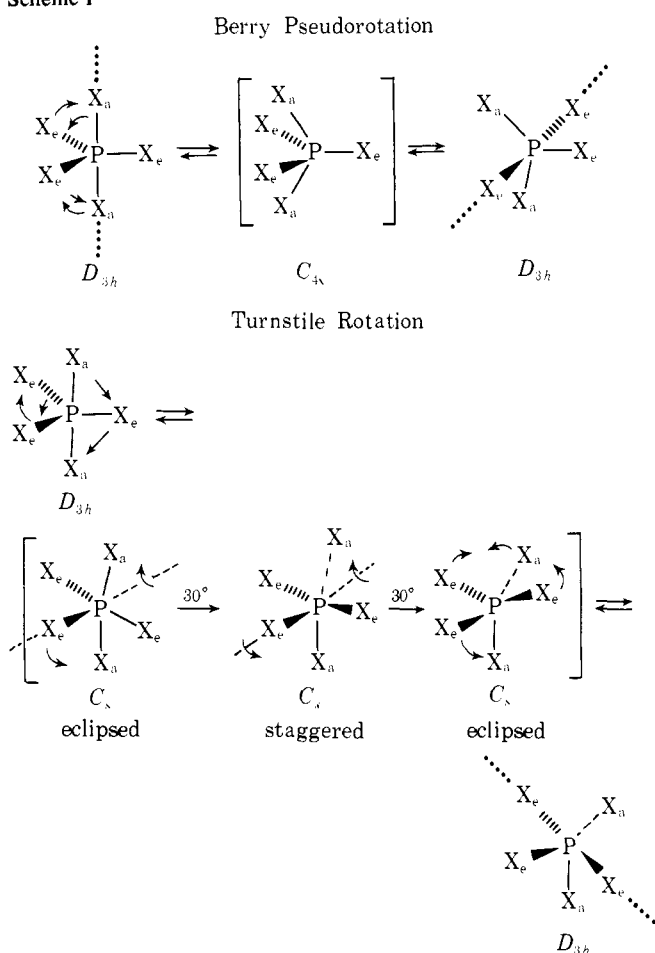
The exchange of ligands around pentacoordinate phosphorus in phosphoranes of the type PX_5 , where X may be aryl or halogen, has been the subject of a wide variety of investigations.¹ Two mechanisms have been proposed to account for the observed exchange: the Berry pseudorotation (BPR)² and the turnstile rotation (TR)³ process as illustrated in Scheme I. Although these mechanistic alternatives involve entirely different molecular motions, it has not been possible hitherto to distinguish between them experimentally.⁴ On the other hand, quantum-mechanical calculations,

both semiempirical⁵ and ab initio,⁶ have shown that the energy of activation for the BPR process is considerably lower than that of the TR process and thus should be favored. However, there has been no attempt so far to investigate the reaction profile of these processes in detail⁷ in order to obtain information with regards to their synchronous or stepwise nature. Furthermore, no consideration has been given to the interrelationship of the TR and BPR modes, which is of considerable importance regarding the experimental distinguishability of these mechanistic alternatives.

Table I. Optimized Geometrical Parameters of PH₅ as a Trigonal Bipyramid (*D*_{3h}), a Tetragonal Pyramid (*C*_{4v}), and a Trigonal Pyramid (*C*_s)

Structure	Symmetry	Bond	Bond length, Å		Symbol	Bond angle, deg		
			X = H	X = F ^b		This work	<i>a</i>	<i>b</i>
	<i>D</i> _{3h}	P-X _a P-X _e	1.577 1.437	1.571 1.542				
	<i>C</i> _{4v}	P-X _a P-X _b	1.406 1.499	1.514 1.561	α	99.57	99.8	101.34
	<i>C</i> _s	P-X _a P-X _b	1.506 1.470	1.55 ^c 1.55 ^c	θ ψ	88.0 92.58	87.2 91.5	85 95

^a Reference 4. EHMO calculations for PH₅. The value of 1.42 Å was assumed for all P-H bonds. ^b Reference 5. Ab initio calculations for PF₅. ^c These are assumed bond lengths.

Scheme I

The objective of this investigation was therefore a thorough theoretical examination of the foregoing aspects using PH₅ as a model molecule.

Computational Details

All computations have been carried out on an IBM 370/165 computer.

The cross sections of the reaction hypersurface were investigated by means of nonempirical LCAO-MO-SCF calculations using the GAUSSIAN 70 program system⁸ and employing a relatively modest split valence shell (4-31G), basis set. The net atomic charges and overlap populations were obtained from Mulliken population analysis.⁹

The vibrational levels were calculated from the ab initio force constant using harmonic approximation.

Results and Discussion

Geometries and Charge Distributions. The present study began with the complete optimization of three distinct geometries corresponding to the *D*_{3h}, *C*_{4v}, and *C*_s (eclipsed) structures. The results are shown in Table I and the corresponding energies are given at the appropriate places in Table II (cf. footnote *a*). The results of EHMO calculations⁵ for PH₅ and the ab initio results for PF₅⁶ are also included in Table I. Direct comparison with these cannot be made since (a) the former employed an assumed P-H bond length for all the structures under consideration, (b) the latter work was for PF₅, and (c) no complete geometry optimization is available at the present time for the *C*_s structure for either PH₅ or PF₅. However, certain general trends are apparent: e.g., in the *D*_{3h} structure, axial bonds are longer than equatorial bonds;¹⁰ in the *C*_{4v} structure, basal bonds are longer than the apical bond. The latter should be contrasted with the results found for the *C*_s structure in which the three equivalent pyramidal P-H bonds are somewhat shorter than the other two equivalent quasi-apical bonds.

The net atomic charges and the overlap populations of the bonds for the three optimized geometries, as well as for the *C*_s (staggered) structure, obtained by a 30° rotation of the X_a ligands (cf. Table I) about the central C₂-C₃ axis, are illustrated in Figure 1. The values obtained for both the *D*_{3h} and the *C*_{4v} geometry are in qualitative agreement with previous reports^{5,11} and reflect the idea of "electron-rich multicenter bonding"⁵ in PH₅. A close examination of the values obtained for both *C*_s structures, however, reveals that the local *C*₃ and *C*₂ symmetry is not apparent at all. In fact, the *C*_s (eclipsed) structure resembles a distorted *D*_{3h} molecule, whereas the *C*_s (staggered) structure resembles a distorted *C*_{4v} molecule.

Similar results were obtained by Hoffmann et al.⁵ for a PH₅ molecule with five identical bonds of assumed length. Since our results were arrived at by complete geometry optimization, the qualitative bonding picture of the above authors has now further been substantiated.

Investigation of the Reaction Profiles. The purpose of this part of the investigation was to examine the energetics of possible sequential processes as alternatives to the concerted pathway in both the BPR and the TR.

In the case of the former, a sequential process could be envisaged as one involving (a) initial equatorial bending followed by axial bending, or (b) initial axial bending followed by equatorial bending, or (c) some combination of (a) and

Table II. Variation of the Total Energy along the Reaction Coordinates Chosen for the BPR and for Modes I, II, and III of the TR Process

Mode	Percent reaction ^e along coordinate	Symmetry	Energy (hartrees)	
BPR	0	D_{3h}^a	-343.025 101 000	
	12.5	C_{2v}^b	-343.024 336 687	
	25.0	C_{2v}^b	-343.023 096 981	
	37.5	C_{2v}^b	-343.022 415 422	
	39.0	C_{2v}^b	-343.022 057 346	
	45.0	C_{2v}^b	-343.022 369 158	
TR I	0	C_{4v}^a	-343.022 381 457	
	12.5	D_{3h}^a	-343.025 101 000	
	12.5	C_c	-343.021 348 984	
	25.0	C_c	-343.011 246 679	
	37.5	C_c	-342.997 430 318	
	50.0	C_s^d	-343.008 653 048	
TR II	0	D_{3h}^a	-343.025 101 000	
	6.25	C_s	-343.024 289 425	
	12.5	C_s	-343.022 342 343	
	18.75	C_s	-343.018 811 572	
	21.9	C_s	-343.011 953 111	
	23.75	C_s	-343.009 193 725	
	25.0	C_s^a	-343.009 090 00	
	50.0	C_s^d	-343.008 653 048	
	TR III	0	D_{3h}^a	-343.025 101 000
		6.25	C_{2v}	-343.024 500 884
12.5		C_{2v}	-343.022 841 941	
18.75		C_{2v}	-343.019 716 875	
25.0		C_{2v}	-343.014 798 220	
31.25		C_c	-343.014 707 111	
37.5		C_c	-343.007 123 351	
43.75		C_c	-342.995 762 837	
50.0		C_s^d	-343.008 653 048	

^a For the optimized geometries, see Table I. ^b Individually optimized points. Geometries are not reported. ^c No geometry optimization is possible for these points since due to the lack of symmetry all points converge to the initial state. ^d Staggered conformation obtained from the optimized eclipsed structure by a 30° rotation about the central C(3)-C(2) axis. ^e Values are reported up till 50% reaction only since the curves are symmetrical about that point.

(b) which becomes the concerted mode in a limiting case, i.e., a synchronous motion of all the atoms towards a C_{4v} structure.

These possibilities were probed in the following way: one of the geometrical parameters was allowed to vary in a linear fashion from the initial (D_{3h}) to the final (C_{4v}) geometry. The remaining parameters were then optimized at various intervals along that path with the restriction that a C_{2v} symmetry has to be maintained throughout. The structural parameters thus obtained were found to vary in proportion to the set parameter. This means that the energetically most favorable situation involves the synchronous movement of all the atoms along the reaction coordinate. The energy profile corresponding to this motion is illustrated in Figure 2A, and the corresponding energy values are given in Table II. The curve appears to be extremely flat with a rather broad plateau but no significant minimum at the midpoint.¹² The calculated barrier to the interconversion is 1.95 kcal/mol, this being in good agreement with both the calculated values of 2.1⁵ and 1.6 kcal/mol, the latter representing an estimate based on vibrational data transferred from a series of pentacoordinated molecules.^{1,13} According to our results, it may be concluded that the BPR should be a concerted process involving a transition state or a transient intermediate¹² of C_{4v} symmetry and a very low energy of activation.

For the TR process three possibilities were considered: (mode I) synchronous movement of all the atoms toward a C_s (staggered) end point structure; (mode II) synchronous

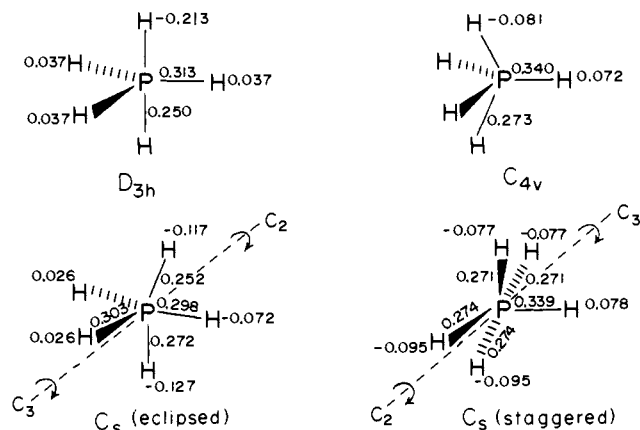


Figure 1. Net charges and bond overlap populations as obtained from Mulliken population analysis.

movement of all the atoms toward a C_s (eclipsed) end point, followed by torsion to a C_s (staggered) conformation; (mode III) initial in-plane equatorial bend followed by synchronous movement of all the atoms toward a C_s (staggered) structure.

These possibilities are schematically illustrated in Figure 3. As is shown, the originally many-dimensional problem is simplified in the present analysis by grouping several degrees of freedom together. The heavy arrows indicate the reaction coordinates chosen for the investigation.

The results obtained for mode I are shown in Figure 2B and the corresponding energy values in Table II. As apparent from the shape of the curve, the synchronous motion in the case of the TR, in contrast to the BPR, involves a barrier of 17.0 kcal/mol.

The cross section corresponding to mode II is illustrated in Figure 2C (cf. Table II for energy values). The energy required for the first part of the sequence is 10.1 kcal/mol. The second part of the sequence, the sixfold torsion about the central C₂-C₃ axis, has a surprisingly high barrier (0.27 kcal/mol), considering that the sixfold rotational barriers are known¹⁴ to be in the neighborhood of a few calories per mole. This is probably due to the fact that that particular investigation¹⁴ refers to models in which rotation was carried out about a bond rather than about a central atom.

Figure 2D shows the cross section corresponding to mode III (cf. Table II for energy values). As was expected, the initial in-plane equatorial bend requires relatively little energy, 6.5 kcal/mol. However, reorganization of the rest of the molecule to attain the C_s (staggered) conformation is even less favorable than the concerted path (mode I). The overall activation energy for this mode is 18.4 kcal/mol.

Based on the above presented results, the most probable pathway for the TR process is mode II.

Thus, the TR process prefers to proceed sequentially rather than in a concerted fashion as in the case of BPR. This preference may be due to the conservation of a plane of symmetry during the first part of mode II. In mode I no symmetry element was conserved along the reaction coordinate; the corresponding energy change was found to be relatively large. The above considerations also apply to mode III in which the removal of the initial plane of symmetry for the synchronous, i.e., the second part of the sequence, resulted in a drastic increase in energy.

A feature relating to the similarity of the shapes of the profiles corresponding to mode II and the BPR is noteworthy. The relatively large plateau and low barrier implies that while the BPR should always be favored when geometry allows, mode II of the TR may be the active reaction coordinate for structurally restricted systems such as¹⁵

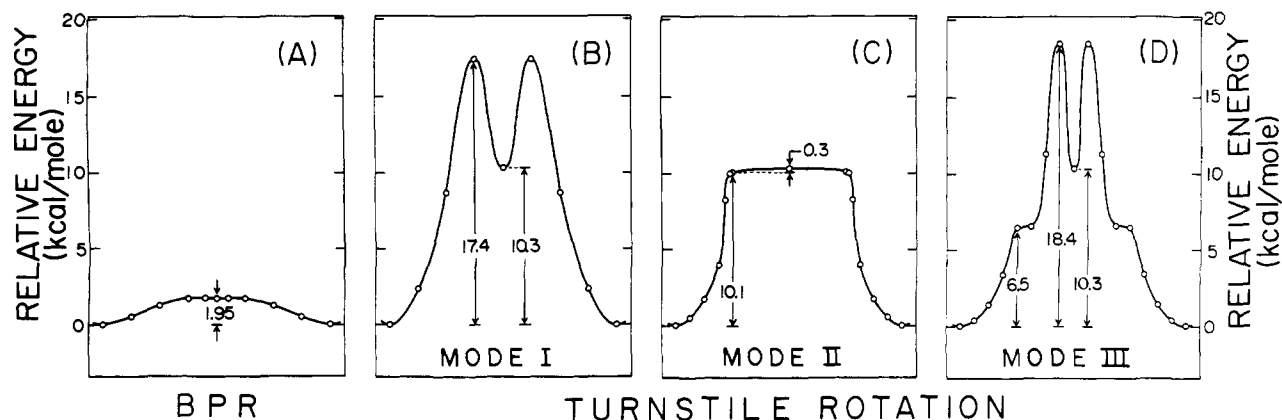


Figure 2. Energy profiles for the pentatopal rearrangement of PH_5 . (A) Berry pseudorotation; (B, C, and D) modes I, II, and III of the turnstile rotation, respectively.

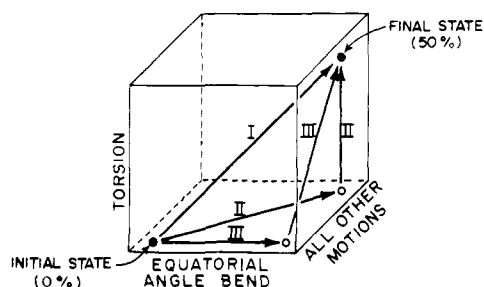
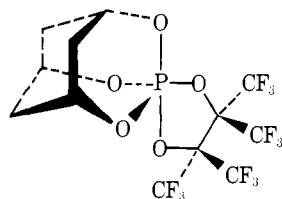


Figure 3. Schematic representation of the combination of internal motions considered for the turnstile rotation process.



since the geometry of such molecules is already distorted¹⁶ toward that path.

Interdependence of BPR and TR mechanisms. In the previous section, comparison was made between the BPR and TR processes, considering them as two distinct mechanistic pathways with corresponding transition states of C_{4v} and C_s (staggered) symmetries, respectively. However, results of the charge distribution studies (discussed earlier in the text) revealed that the C_s (staggered) structure resembles a distorted C_{4v} -type species. The question, therefore, which remained to be answered was: what is the shape of that cross section of the reaction hypersurface which interconnects the C_{4v} and C_s species?

Our results for this cross section are shown in Figure 4. As is apparent, the energy increases monotonically as the C_{4v} symmetry is distorted toward the hypothetical transition state of the TR process. The curve is nearly parabolic and relatively steep; the harmonic one-dimensional oscillator levels are separated by 1.32 kcal/mol so that 99.9% of the population is at the ground and first two vibrationally excited states at room temperature.¹⁷ Since the energy corresponding to the C_s symmetry species is higher than the sixth excited vibrational level (cf. Figure 4), this species can be regarded as arising from the C_{4v} structure by vibrational excitation at high temperature.

The calculated harmonic force constant for the distortion is 0.15 mdyne/Å. Comparing this value with the in-plane equatorial PX_2 bending (0.32 mdyne/Å) and axial PX_2'

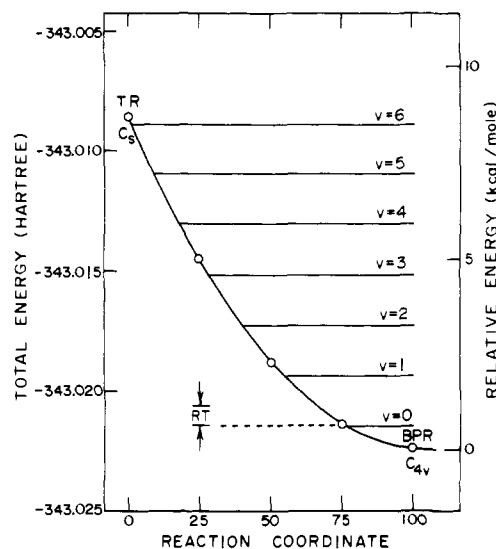


Figure 4. Potential curve interconnecting the C_s and C_{4v} species. The calculated harmonic vibrational levels are also shown.

bending (0.083 mdyne/Å) force constants predicted for PH_5 by Holmes et al.,¹³ it appears that the distortion is some combination of bending vibrational modes of the molecule.

In conclusion, it appears from the present study that, at least in the case of structurally flexible phosphoranes, as modeled by PH_5 , the TR mode is not a distinctly different mechanistic pathway, but in fact a vibrationally excited mode of the BPR. This is based on our observation that the C_s (staggered) conformation does not appear on the reaction hypersurface as a distinct saddle point. If this is really the case, then the BPR and TR modes are, in fact, indistinguishable experimentally.

Acknowledgment. The authors gratefully acknowledge the continued support of the National Research Council of Canada.

References and Notes

- (1) Several reviews are available on this topic; see, for example, R. R. Holmes, *Acc. Chem. Res.*, **5**, 296 (1972), and references therein.
- (2) R. S. Berry, *J. Chem. Phys.*, **32**, 933 (1960).
- (3) I. Ugi, D. Marquarding, H. Klusacek, P. Gillespie, and F. Ramirez, *Acc. Chem. Res.*, **4**, 288 (1971).
- (4) P. Meakin, A. D. English, S. D. Ittel, and J. P. Jesson, *J. Am. Chem. Soc.*, **97**, 1254 (1975).
- (5) R. Hoffmann, J. M. Howell, and E. L. Muetterties, *J. Am. Chem. Soc.*, **94**, 3047 (1972).
- (6) A. Strich and A. Veillard, *J. Am. Chem. Soc.*, **95**, 5574 (1973).
- (7) D. Britton and J. D. Dunitz, *J. Am. Chem. Soc.*, **97**, 3836 (1975).

- (8) W. J. Hehre, W. A. Lathan, R. Ditchfield, M. D. Newton, and J. A. Pople, GAUSSIAN 70, QCPE Program No. 236, Quantum Chemistry Program Exchange, Indiana University.
- (9) R. S. Mulliken, *J. Chem. Phys.*, **23**, 1833, 1841, 2338, 2343 (1955).
- (10) This has been observed for a series of trigonal-bipyramidal molecules; see, for example, ref 1.
- (11) A. Rauk, L. C. Allen, and K. Mislow, *J. Am. Chem. Soc.*, **94**, 3035 (1972).
- (12) The energy of the structure obtained at 45% reaction was found to be 0.005 kcal/mol higher than that of the C_{4v} structure even after double cycle optimization (cf. Table II).
- (13) R. R. Holmes, Sr., R. M. Deiters, and J. A. Golen, *Inorg. Chem.*, **8**, 2612 (1969).
- (14) L. M. Tel. S. Wolfe, and I. G. Csizmadia, *Int. J. Quantum Chem.*, **7**, 475 (1973).
- (15) I. Ugi, F. Ramirez, D. Marquarding, H. Klusacek, G. Gokel, and P. Gillespie, *Angew. Chem., Int. Ed. Engl.*, **9**, 725, (1970).
- (16) H. L. Carrell, H. M. Berman, J. S. Ricci, Jr., W. C. Hamilton, F. Ramirez, J. F. Marecek, L. Kramer, and I. Ugi, *J. Am. Chem. Soc.*, **97**, 38 (1975).
- (17) The following Boltzman distribution values were obtained from the populations of the 0th, 1st, and 2d vibrational levels: 89.2, 9.6, 1.1%, respectively.

Mercury $6(^3P_1)$ Photosensitization of Trifluoroethylene. A Source of the Difluorovinylidene Carbene

R. J. Norstrom,¹ H. E. Gunning, and O. P. Strausz*

Contribution from the Department of Chemistry, University of Alberta, Edmonton, Alberta, Canada. Received May 12, 1975

Abstract: The triplet mercury photosensitization of trifluoroethylene proceeds via an excited molecule mechanism leading to the geminal molecular elimination of HF and the novel difluorovinylidene carbene with a zero-pressure extrapolated quantum yield of ≥ 0.8 . An additional minor primary step is C=C bond cleavage giving :CF₂ and :CFH. Decomposition probably occurs from the excited triplet state of C₂HF₃, and the ethylidene structure is not implicated in the mechanism. Difluorovinylidene is formed in its singlet ground state and adds readily across the double bond of the parent olefin to give a hot difluoromethylene-trifluorocyclopropane which decomposes to :CF₂ + CF₂=C=CHF or, if partially pressure stabilized, isomerizes to CF₂=CHCF=CF₂. Difluorovinylidene also reacts with paraffins via direct insertion into the C-H bond but does not react with molecular oxygen or carbon monoxide.

In a previous publication on the Hg $6(^3P_1)$ photosensitized decomposition of mono- and difluorinated ethylenes,² it was shown that decomposition proceeds via an excited molecule mechanism by molecular elimination of HF. From a comparison of the experimental rate constants for the isomerization and decomposition reactions of ethylene, vinyl chloride, mono-, di-, and trifluoroethylenes with those computed with the aid of the RRK formula, it was concluded that intervention of the isomeric ethylidene structure in the decomposition mechanism is possible in all cases except with trifluoroethylene and 1,2-difluoroethylene. The estimated energy levels of the triplet ethylidene states of these latter molecules would lie so high that the rate constant for triplet ethylene \rightarrow triplet ethylidene isomerization would be lower than the experimental rate constant for the overall decomposition. The RRK calculations employed were based on an empirical estimate of the triplet ethylene and ethylidene state energy levels derived from extended Hückel MO calculations.

The present article reports the determination of the experimental rate constant for the overall decomposition of trifluoroethylene and discusses the mechanistic details of the reaction.

Experimental Section

The apparatus and general experimental technique employed were similar to those described in the previous article.² Trifluoroethylene (Peninsular) was distilled from ethyl chloride slush (-139°) and purified by gas chromatography. O₂ and CO were Airco Assayed Reagent Grade and were used without purification. Propane-*d*₈ and cyclohexane-*d*₁₂ were from Merck, C₃H₈ and CF₄ from Matheson, and cyclohexane from Phillips. They were degassed and purified by low-temperature distillation.

Analyses of the reaction mixtures were accomplished by combination of low-temperature distillation and gas-chromatographic separation. The reaction mixtures from the pure C₂HF₃ experiments were analyzed on a 28-ft 10% diisodecyl phthalate on Dia-

toport column at 25°. The substrate and C₂ products were trapped from the effluent and quantitatively analyzed on a 4-ft high-activity silica gel column at 50°. In experiments with added CF₄, the excess CF₄ was removed by distillation at liquid oxygen temperature (-183°). Similarly, with added O₂ or CO, the excess noncondensables were removed by pumping at -196° , and the reaction mixture was analyzed as above. In experiments with added propane, the analysis was accomplished as with pure C₂HF₃. In the case of added cyclohexane, the C₂ and C₃ compounds were distilled from the reaction mixture at -130° and analyzed as before. The remainder, consisting of the added cyclohexane and new reaction products, was analyzed on a 6-ft 20% di-*n*-nonyl phthalate on firebrick column at 25°.

Results

The products found were 1,1,2,4,4-pentafluorobutadiene (C₄HF₅), trifluoroallene (C₃HF₃), and tetrafluoroethylene (C₂F₄). C₂F₄ was identified by mass spectrometry. The mass spectrum of C₃HF₃, compiled in Table I, gave a large parent peak at *m/e* 94, and the ir spectrum, shown in Figure 1a, had a strong absorption band at 2040 cm⁻¹, the usual region for allenic type C=C stretching. The ir spectrum of 1,1-difluoroallene³ also has a strong band at 2040 cm⁻¹. The NMR spectrum of C₃HF₃ exhibited two doublets, removed from one another by 87 Hz, with a splitting within the doublets of ca. 1 Hz. It is known that geminal H-F coupling in olefinic systems is very large, for example, 84.8 Hz in *cis*-1-fluoro-1-propane.⁴ The small splitting is due to long range coupling to the fluorines on the other end of the molecule. Any other isomer of empirical formula C₃HF₃ would have exhibited a singlet or a triplet spectrum. The chemical shift of τ 2.92 is in the aromatic proton region, which is consistent with the shift to lower than normal field due to the presence of geminal fluorine.

Identification of the C₄HF₅ product was considerably more difficult. High-resolution mass spectra (Table I) were obtained at four different electron energies. From the varia-